JOURNAL OF GUIDANCE, CONTROL, AND DYNAMICS
Vol. 23, No. 1, January–February 2000

Postcapture Dynamics of a Spacecraft-Manipulator-Payload System

Xavier Cyril*
CAE Electronics, Ltd., St. Laurent, Quebec H4L 4X4, Canada
Arun K. Misra† and Michel Ingham‡
McGill University, Montreal, Quebec H3A 2K6, Canada
and
Gilbert J. Jaar§
CAE Electronics Ltd., St. Laurent, Quebec H4L 4X4, Canada

Space manipulators will play an increasingly significant role in future space operations. They will handle payloads of varying geometric or physical properties depending on their missions. In the ideal case, the manipulator should approach the payload in such a manner that, at the time of capture, the relative velocity between the end-effector and the payload grapple point is zero. Then the capture will be without impact and a smooth one. In practice, however, this is not likely, and there will be a nonzero relative velocity between the end effector and the payload grapple point, leading to an impact. In this paper we study the dynamics of the manipulator, the mother spacecraft, and the payload after such a capture with an impact. The dynamic models of the spacecraft-manipulator system before capture and spacecraft-manipulator-payload system after capture are obtained using the Lagrangian formulation. An impact model is developed to calculate the changes in the generalized velocities caused by the impact. These are then used as initial conditions for simulation of the postimpact dynamics of the combined spacecraft-manipulator-payload system. Both rigid and flexible payloads are considered. The simulations show that the dynamics response can be significantly different depending on whether the capture is smooth or with an impact and whether the payload is flexible or rigid. If the dynamics are uncontrolled, the response can be undesirably large; a control scheme based on feedback linearization is proposed to avoid this.

Introduction

IN recent years there has been an increasing interest in the application of space robotics. Space manipulators will play a significant role in future space operations. They will be used for assembly and fabrication of space structures required for the construction of the proposed space station. Currently the shuttle-mounted manipulator is used in conjunction with astronaut extra vehicular activity (EVA) for the inspection, repair, and (if necessary) retrieval of malfunctioning satellites. The future goal is to minimize the need for EVA, which would greatly reduce both mission costs and hazards to the astronauts involved. Berthing of two spacecraft (e.g., shuttle to the space station) could also take place through a manipulator.

In all of the just-mentioned robotic operations, the manipulator undergoes several phases of dynamics, namely, approach dynamics, contact dynamics, and residual motion dynamics. The success or failure of these robotic operations greatly depends on the physical processes involved in the operation and the ability to control these processes. Toward this end, several researchers have attempted to understand the space robotic operations through dynamic modeling and simulation. Umetani and Yoshida[1,2] used the momentum conservation laws and introduced the concept of the Generalized Jacobian Matrix to control free-flying manipulators, taking into account the effects of the dynamic coupling between a robot and its base on the positioning of the end-effector and on the relative position and orientation of the spacecraft. The effect of structural flexibility inherent in the links has also been investigated quite extensively. Longman[3] concluded that the induced vibrations resulting from the elasticity could be so substantial that they might tumble the spacecraft on which the manipulator is mounted. The complexity arising from incorporating the flexibility in the dynamic modeling has led many researchers simply to ignore its effects. However, this can lead to a substantial deterioration of the tracking accuracy. Baruh and Tadikunda[4] treated the flexibility effect as a deterministic disturbance on the rigid body motion. Consequently, the flexible motion could be treated similarly to the way the gravitational, Coriolis, and centrifugal effects are treated.

As a result of the undesirable movements of the system's components resulting from performing a task, control is usually required for space manipulators. Several researchers have investigated control issues, but most of them assumed that the base of the manipulator is stationary. On the other hand, it was shown by Papadopoulos and Dubowsky[5] that nearly any control algorithm that can be used for fixed-base manipulators can also be implemented on free-floating space robots, provided that the platform's position and attitude are estimated and taken into account in the design. Dubowsky et al.[6] proposed the use of reaction wheels and/or jet thrusters to control the spacecraft's attitude and position by compensating for the forces and moments exerted on the robot base as a result of the motion. This control scheme enables the designer to use the control schemes designed for terrestrial robots. However, reaction jets may consume large amounts of expensive fuel and hence limit the useful life of the system as suggested by Torres and Dubowsky.[7] Longman et al.[8] suggested the control of the spacecraft's attitude only, which leaves the spacecraft free to translate in response to the force disturbances of the robot and the payload. This control scheme is far more complicated than the one presented by Dubowsky et al.[6]; however, it could be simplified by using the virtual manipulator technique presented in Ref. 9. All of the just-mentioned researchers were mainly concerned with the control of free-floating space robots in the process of capturing a payload. Not much attention has been given toward analyzing the effect of the impact after capture on the subsequent behavior of the system.

When contact occurs, impact dynamics can be a significant factor. If impact forces are not modeled, and if the resulting movements of the manipulator are not controlled to prevent inappropriate forces, the robotic operation may fail. Wang and Mason[10] considered

Received 20 May 1996; revision received 15 July 1997; accepted for publication 20 May 1999.

*Manager, P.O. Box 1800, Space Systems Engineering.
†Professor, Department of Mechanical Engineering, 817 Sherbrooke Street West. Associate Fellow AIAA.
‡Research Assistant, Department of Mechanical Engineering, 817 Sherbrooke Street West.
§Engineer, P.O. Box 1800, Space Systems Engineering.

the impact of two objects in planar motion and presented a simple graphical method for predicting the mode of contact and the resultant motion of the objects. The use of extended generalized inertia tensor and the virtual mass concepts to formulate the collision problem was demonstrated by Yoshida et al.[11] This work focuses on the velocity relationship before and after the collision of two rigid systems. Yoshida[12] has also presented the dynamics simulation results that reveal the effects of impact on the rigid body system. However, none of the just-mentioned researchers have considered the collision of a flexible manipulator with a flexible payload, although dynamics modeling of a flexible arm holding a flexible payload has been presented by Carton et al.[13] Cyril et al.[14] studied the dynamics and control associated with capture of a spinning satellite; however, the assumption was made that at the time of capture there is zero relative velocity between the payload and the end-effector of the manipulator—in other words, there is no impact. In this paper the dynamics of a spacecraft-mounted manipulator (modeled as flexible) capturing a flexible payload (e.g., satellite with an appendage) with an impact is studied, and their postcapture dynamics is simulated.

Spacecraft-Manipulator Dynamics Model

The dynamic equations of a spacecraft-manipulator system have been derived by several investigators and will not be discussed further. The model used in this paper is developed in Cyril et al.[15] and can be expressed in the form

$$\boldsymbol{M}\,\ddot{\psi} = \boldsymbol{c}(\Psi, \dot{\Psi}, \Psi_0) + \boldsymbol{f} \tag{1}$$

In the preceding equation $\boldsymbol{M}$ is the generalized mass matrix of the system, which is symmetric and positive definite. Vector $\boldsymbol{f}$ represents the generalized external forces, the vector $\boldsymbol{c}$ contains the Coriolis, damping, and centrifugal terms, Ψ is the vector of generalized coordinates, $\dot{\Psi}$ is the generalized velocity vector, and Ψ_0 is the vector containing the orbital rate of the system.

Impact Dynamics Model

To determine the initial conditions for the postimpact simulation, let us suppose that an M-body payload impacts the end effector of an N-body spacecraft-mounted manipulator. During this impact, the equations of motion of the spacecraft manipulator and payload respectively can be written as follows:

$$\boldsymbol{M}\dot{\Psi} = \boldsymbol{c} + \boldsymbol{f} + \boldsymbol{J}^T\boldsymbol{f}_c \tag{2}$$

$$\boldsymbol{M}_p\dot{\Psi}_p = \boldsymbol{c}_p + \boldsymbol{f}_p - \boldsymbol{J}_p^T\boldsymbol{f}_c \tag{3}$$

where $\Psi_p, \boldsymbol{J}, \boldsymbol{J}_p$, and $\boldsymbol{f}_c$ are respectively the generalized velocity vector of the payload, the Jacobian of the spacecraft manipulator, the Jacobian of the payload, and the generalized force vector due to the impact force arising during the capture of the payload by the spacecraft-manipulator system.

The $(6 \times N')$ Jacobian $\boldsymbol{J}$ of the elastic multibody system can be written as

$$\boldsymbol{J} = \begin{bmatrix} \boldsymbol{J}_1 \\ \boldsymbol{J}_2 \end{bmatrix} \tag{4}$$

where

$$\boldsymbol{J}_1 = \left[\frac{\partial \boldsymbol{p}_h}{\partial \psi_1} \cdots\cdots \frac{\partial \boldsymbol{p}_h}{\partial \psi_{N'}} \right] \tag{5}$$

$$\boldsymbol{J}_2 = [\boldsymbol{y}_1 \cdots\cdots \boldsymbol{y}_N] \tag{6}$$

in which

$$\boldsymbol{y}_j = \boldsymbol{e}_j, \qquad \text{if } j\text{th body is rigid}$$

$$\boldsymbol{y}_j = \left[\boldsymbol{e}_j \sum_j \frac{\partial \zeta_j}{\partial \boldsymbol{x}_i}\boldsymbol{x}_i \sum_k \frac{\partial \eta_k}{\partial \boldsymbol{x}_i}\boldsymbol{y}_i \sum_s \frac{\partial \xi_s}{\partial \boldsymbol{x}_i}\boldsymbol{z}_i \right], \qquad \text{if } j\text{th body is flexible} \tag{7}$$

Here N' is the total number of degrees of freedom in the elastic multibody system, $\boldsymbol{p}_h$ respresents the position vector of the point of impact of the multibody system with respect to body-1 frame, $\boldsymbol{e}_j$ represents the unit vector along the axis of the jth rigid degree of freedom, whereas ζ_j, η_k, and ξ_s are the shape functions used to describe the in-plane bending, out-of-plane bending, and torsional deformations, respectively.

The expression for $\boldsymbol{J}_p$ can be written in an analogous manner.

By combining the two equations of motion (2) and (3), the impact force vector $\boldsymbol{f}_c$ can be eliminated to yield the following equation:

$$\boldsymbol{J}^T\boldsymbol{P}^{-1}\boldsymbol{J}_p\boldsymbol{M}_p\dot{\Psi}_p + \boldsymbol{M}\dot{\Psi} = \boldsymbol{c} + \boldsymbol{f} + \boldsymbol{J}^T\boldsymbol{P}^{-1}\boldsymbol{J}_p(\boldsymbol{c}_p + \boldsymbol{f}_p) \tag{8}$$

where

$$\boldsymbol{P} = \boldsymbol{J}_p\boldsymbol{J}_p^T \tag{9}$$

Note that $\boldsymbol{J}_p$ in general can be a rectangular matrix, which does not have an inverse, but $\boldsymbol{P}$ does.

Now before integrating the preceding equation over the period T, one can recall the assumption that all of the generalized coordinates of the system remain fixed during this period, although their rates may change. Because $\boldsymbol{J}$, $\boldsymbol{J}_p$, $\boldsymbol{M}_p$, and $\boldsymbol{M}$ depend only on the former and not on the latter, these matrices can be taken out of the integral. Also, the impact force is usually very large and acts for a very short time T. Thus one can say that

$$\begin{aligned} \boldsymbol{T} &= \mathcal{O}(\epsilon), \qquad \epsilon \ll 1 \\ \Psi, \Psi_p, \dot{\Psi}, \dot{\Psi}_p &= \mathcal{O}(1) \\ \dot{\Psi}, \dot{\Psi}_p &= \mathcal{O}(1/\epsilon) \end{aligned} \tag{10}$$

Now, integration of Eq. (8) yields:

$$\boldsymbol{J}^T\boldsymbol{P}^{-1}\boldsymbol{J}_p\,\boldsymbol{M}_p(\dot{\Psi}_{\mathrm{pf}} - \dot{\Psi}_{\mathrm{pi}}) + \boldsymbol{M}(\dot{\Psi}_f - \dot{\Psi}_i) = \int_0^T \left[\boldsymbol{c} + \boldsymbol{f} + \boldsymbol{J}^T\boldsymbol{P}^{-1}\boldsymbol{J}_p(\boldsymbol{c}_p + \boldsymbol{f}_p)\right] \mathrm{d}t \tag{11}$$

where the subscripts f and i stand for values after and before the impact, respectively. Clearly, the left-hand side of Eq. (11) is $\mathcal{O}(1)$. The integrand on the right-hand side is also $\mathcal{O}(1)$; however, the interval of the integration is of $\mathcal{O}(\epsilon)$ and, hence, the right-hand side is of $\mathcal{O}(\epsilon)$ and can be ignored compared to the left-hand side. Thus Eq. (11) becomes

$$\boldsymbol{J}^T\boldsymbol{P}^{-1}\boldsymbol{J}_p\boldsymbol{M}_p(\dot{\Psi}_{\mathrm{pf}} - \dot{\Psi}_{\mathrm{pi}}) + \boldsymbol{M}(\dot{\Psi}_f - \dot{\Psi}_i) = 0 \tag{12}$$

Equation (12) represents conservation of generalized momenta and is applicable to all collisions ranging from plastic to perfectly elastic. In the case of plastic impact, the two systems become rigidly attached to each other after impact at the contact points, whereas in the case of elastic impact, the systems rebound with no loss of energy. The former case corresponds to successful capture or berthing.

In plastic impact the velocity of the contact point of each system is the same immediately after the impact. Thus, one obtains

$$\boldsymbol{J}_p\dot{\Psi}_{\mathrm{pf}} = \boldsymbol{J}\dot{\Psi}_f \tag{13}$$

One can then solve the generalized velocities of the target in terms of those of the chaser to obtain

$$\dot{\Psi}_{\mathrm{pf}} = \boldsymbol{Q}^{-1}\boldsymbol{J}_p^T\boldsymbol{J}\dot{\Psi}_f \tag{14}$$

where

$$\boldsymbol{Q} = \boldsymbol{J}_p^T\boldsymbol{J}_p \tag{15}$$

Substitution of Eq. (14) into Eq. (12) yields

$$\dot{\Psi}_f = \boldsymbol{G}^{-1}\boldsymbol{H} \tag{16}$$

where

$$\begin{aligned} \boldsymbol{G} &= \boldsymbol{J}^T\boldsymbol{P}^{-1}\boldsymbol{J}_p\boldsymbol{M}_p\boldsymbol{Q}^{-1}\boldsymbol{J}_p^T\boldsymbol{J} + \boldsymbol{M} \\ \boldsymbol{H} &= \boldsymbol{J}^T\boldsymbol{P}^{-1}\boldsymbol{J}_p\boldsymbol{M}_p\dot{\Psi}_{\mathrm{pi}} + \boldsymbol{M}\dot{\Psi}_i \end{aligned} \tag{17}$$

Once $\dot{\Psi}_f$ for the spacecraft-manipulator system has been determined, one can use Eq. (14) to evaluate $\dot{\Psi}_{\mathrm{pf}}$ for the payload.

Equations (14) and (16) hold good for any two flexible multibody systems undergoing a plastic impact and can be used as long as $\boldsymbol{P}$ and $\boldsymbol{Q}$ are nonsingular.

A special case of interest is when one of the systems is a rigid body. This situation occurs when the shuttle/manipulator system captures a disabled, basically rigid satellite or when the space station/manipulator system docks with the shuttle. From the postimpact dynamics simulation point of view, it is immaterial as to which system has an active trajectory control. For our analysis the rigid body is termed the target payload.

If the payload is a single rigid body, Eq. (3) can be written as

$$\boldsymbol{M}_p \dot{\boldsymbol{w}}_p = \boldsymbol{f}_p - \boldsymbol{A}\xi_c \tag{18}$$

where $\boldsymbol{w}_p$ is the six-dimensional extended velocity vector consisting of the velocity of the center of mass and the angular velocity components and $\boldsymbol{M}_p$ is the extended mass matrix that can be written as

$$\boldsymbol{M}_p = \begin{bmatrix} m_p \boldsymbol{I} & 0 \\ \boldsymbol{0} & \boldsymbol{I}_p \end{bmatrix} \tag{19}$$

where m_p is the mass of the payload, $\boldsymbol{I}$ is the 3×3 unit matrix, and $\boldsymbol{I}_p$ is the centroidal inertia matrix, while ξ_c is a 6×1 vector consisting of $\boldsymbol{f}_c$ appearing in Eqs. (2) and (3) and a 3×1 zero vector. Furthermore, $\boldsymbol{A}$ can be expressed as

$$\boldsymbol{A} = \begin{bmatrix} \boldsymbol{I} & 0 \\ \boldsymbol{R}_{\text{pb}} & \mathbf{I} \end{bmatrix} \tag{20}$$

where $\boldsymbol{I}$ is the 3×3 unit matrix and $\boldsymbol{R}_{\text{pb}}$ is the cross-product tensor of $\boldsymbol{r}_{\text{pb}}$, which is the position vector of the payload's contact point with respect to its center of mass.

The postimpact generalized velocity vector Ψ_f of the manipulator-carrying spacecraft is again given by Eq. (16), except that $\boldsymbol{G}$ and $\boldsymbol{H}$ now have the following forms:

$$\boldsymbol{G} = m_p \boldsymbol{J}^T \boldsymbol{K}^{-1} \boldsymbol{J} + \boldsymbol{M} \tag{21}$$

$$\boldsymbol{H} = -m_p \boldsymbol{J}^T \left[\boldsymbol{K}^{-1} (-m_p \boldsymbol{R}_{\text{pb}} \boldsymbol{I}_p^{-1} \boldsymbol{R}_{\text{pb}} \boldsymbol{v}_{\text{pi}} + \boldsymbol{R}_{\text{pb}} \omega_{\text{pi}}) - \boldsymbol{v}_{\text{pi}} \right] + \boldsymbol{M} \Psi_i \tag{22}$$

where

$$\boldsymbol{K} = \boldsymbol{I} - m_p \boldsymbol{R}_{\text{pb}} \boldsymbol{I}_p^{-1} \boldsymbol{R}_{\text{pb}} \tag{23}$$

The velocity of the center of mass of the rigid body and its angular velocity just after the impact are given by

$$\boldsymbol{v}_{\text{pf}} = \boldsymbol{K}^{-1} (\boldsymbol{J} \Psi_f - m_p \boldsymbol{R}_{\text{pb}} \boldsymbol{I}_p^{-1} \boldsymbol{R}_{\text{pb}} \boldsymbol{v}_{\text{pi}} + \boldsymbol{R}_{\text{pb}} \omega_{\text{pi}}) \tag{24}$$

$$\omega_{\text{pf}} = m_p \boldsymbol{I}_p^{-1} \boldsymbol{R}_{\text{pb}} (\boldsymbol{v}_{\text{pf}} - \boldsymbol{v}_{\text{pi}}) + \omega_{\text{pi}} \tag{25}$$

Hence, from the preimpact conditions Ψ_f can be calculated using Eqs. (16) and (21–23), and subsequently $\boldsymbol{v}_{\text{pf}}$ and ω_{pf} can be calculated, in that order, using Eqs. (24) and (25).

Control Scheme

As will be seen in the next section, the postimpact motion can be undesirably large. A control scheme is proposed here to avoid large motion. The feedback linearization method is used. The torques are applied by actuating motors in the manipulator joints, and jet-thrusters or reaction wheels in the case of the mother spacecraft.

The dynamics of the combined spacecraft-manipulator-payload system can be written by an equation having the same form as Eq. (1); however, for control purposes it is rearranged as

$$\begin{bmatrix} \boldsymbol{M}_{\theta\theta} & \boldsymbol{M}_{\theta b} \\ \boldsymbol{M}_{b\theta} & \boldsymbol{M}_{bb} \end{bmatrix} \begin{bmatrix} \ddot{\theta} \\ \ddot{\boldsymbol{b}} \end{bmatrix} = \begin{bmatrix} \boldsymbol{c}_\theta \\ \boldsymbol{c}_b \end{bmatrix} + \begin{bmatrix} \tau \\ 0 \end{bmatrix} \tag{26}$$

where θ is the vector of attitude angles of the spacecraft and joint angles of the manipulator and $\boldsymbol{b}$ is the vector of elastic generalized coordinates. One can now eliminate $\ddot{\boldsymbol{b}}$ from Eq. (26) by solving for it from the second set of equations and substituting in the first set to obtain

$$\hat{\boldsymbol{M}} \ddot{\theta} = \hat{\boldsymbol{c}}(\Psi, \Psi, \Psi_0) + \tau \tag{27}$$

where

$$\hat{\boldsymbol{M}} = \boldsymbol{M}_{\theta\theta} - \boldsymbol{M}_{\theta b} \boldsymbol{M}_{bb}^{-1} \boldsymbol{M}_{b\theta} \tag{28}$$

$$\hat{\boldsymbol{c}} = \boldsymbol{c}_\theta - \boldsymbol{M}_{\theta b} \boldsymbol{M}_{bb}^{-1} \boldsymbol{c}_b \tag{29}$$

An appropriate feedback linearization control torque τ is given by

$$\tau = -\hat{\boldsymbol{M}} [\boldsymbol{D}_1 \dot{\theta} + \boldsymbol{D}_2 (\theta - \theta_d)] - \hat{\boldsymbol{c}} \tag{30}$$

where

$$\boldsymbol{D}_1 = \text{diag}(2\zeta_1 \omega_1, 2\zeta_2 \omega_2, \ldots), \qquad \boldsymbol{D}_2 = \text{diag}(\omega_1^2, \omega_2^2, \ldots) \tag{31}$$

are diagonal matrices containing the desired frequency and damping characteristics. Note that the application of the torques given by Eq. (30) reduces Eq. (27) to a set of linearized, uncoupled and homogeneous equations:

$$\ddot{\theta} + \boldsymbol{D}_1 \dot{\theta} + \boldsymbol{D}_2 (\theta - \theta_d) = 0 \tag{32}$$

The control scheme just proposed is a fairly simple one that assumes the availability of all of the states and neglects any noise. A detailed analysis of various control issues is beyond the scope of the present paper.

Simulation Results and Discussion

The system shown in Fig. 1 is chosen as an example for simulation. It is composed of the spacecraft that serves as a platform on which a three-link robotic manipulator is mounted; the first two links are flexible, whereas the third one is a small rigid link containing the end effector. When the satellite is captured successfully by the end effector, it becomes a part of the third link. The orbital and system frames are located at the center of mass C_s of the spacecraft. At a given instant the orientation of the body-fixed frame (X_1, Y_1, Z_1) relative to the orbital frame (X_0, Y_0, Z_0) defines the spacecraft's attitude, represented by the pitch, roll, and yaw angles. The angular velocity of the orbital frame with respect to the inertial frame (X_i, Y_i, Z_i) located at the Earth's center is denoted by Ω. The manipulator is in the process of capturing a malfunctioning satellite. Although the model is three-dimensional, the examples considered here are planar for ease of understanding of the effects of impact.

Three scenarios are considered in this paper. In the first scenario the captured satellite is modeled as a rigid cylinder. For the postimpact simulation the satellite becomes part of body-four of the spacecraft-manipulator system. In the second scenario the satellite is modeled as a rigid cylinder with a flexible appendage. In this

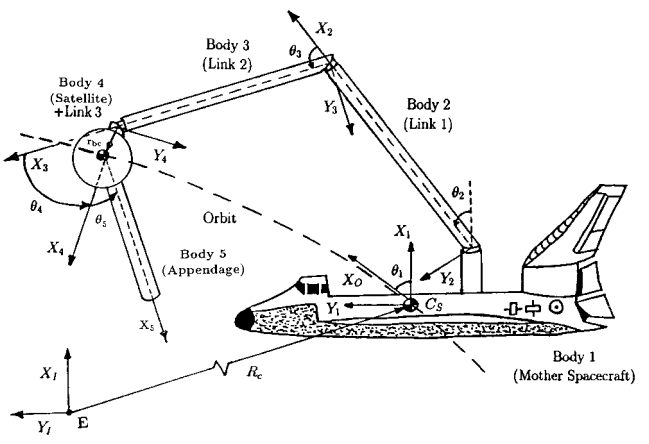

Fig. 1 Spacecraft-manipulator-payload system.

Table 1 Postimpact parameters for the satellite-capture simulation

Body	l, m	m, kg	EI, N-m^2	J_{zz}, kg-m^2
1	n/a	10,000	n/a	40,000
2	8.13	20	881	440.65
3	8.13	20	881	440.65
4	n/a	1,000	n/a	500
5	10	24.6	881	820

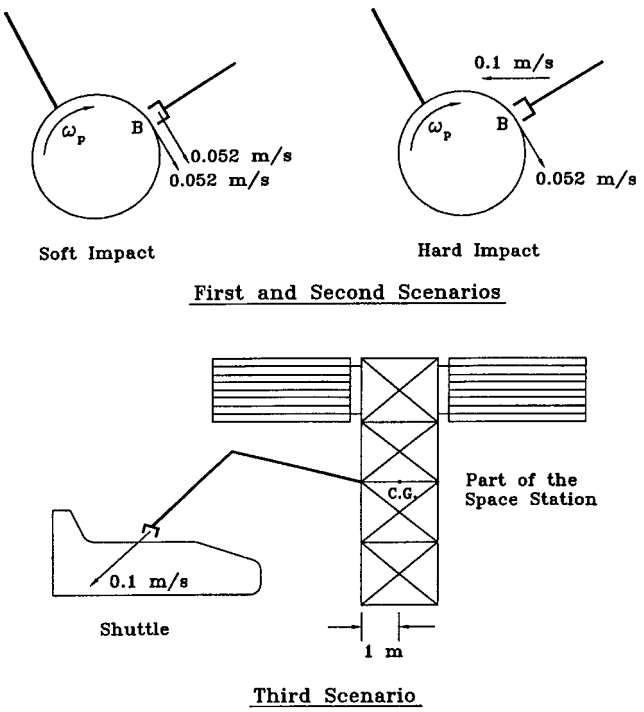

Fig. 2 Definition of the three scenarios.

scenario the satellite becomes part of body-four, whereas the appendage is modeled as body-five. In the last scenario manipulator-assisted berthing of the shuttle with the space station in its early phase is considered. The manipulator in the first two scenarios is representative of the Shuttle Remote Manipulator System (SRMS). The parameters of the simulated system for the first two scenarios are presented in Table 1. The two long booms of the SRMS and the flexible appendage are modeled as elastic with one cantilevered bending mode each; inclusion of additional modes was found to have a small effect. The structural damping was assumed to be 2% of critical damping. In the simulations presented here the objective is to determine the effect of payload impact on the subsequent dynamics of the spacecraft-manipulator-payload system. Therefore, the results presented here are from the postimpact dynamics simulation whose initial conditions are determined using the model given in the impact dynamics model section. In the first scenario (Fig. 2) the manipulator is attempting to capture the payload spinning at the rate $\omega_p = 0.5$ rpm. We consider the two impact cases and compare their results in Fig. 3. The soft-impact case is the one where the velocity of the end effector and that of the point of contact on the payload are the same in magnitude (0.052 m/s) and have the same direction at the time of contact. In the hard-impact case the spacecraft impacts the payload with 0.1 m/s at 112.7 deg to the tangential velocity (0.052 m/s) of the payload. For the hard-impact case two different simulations were conducted, one with the assumption that the manipulator can be modeled as rigid during the short period of impact (rigid impact) and the other where the manipulator is modeled as flexible during impact (flexible impact). The initial conditions for postimpact simulation, as obtained from the impact model, were quite different for the rigid impact and flexible impact cases. Hence, the manipulator should be modeled as flexible not only during the postimpact simulation, but also during the short impact period; this was done for all of the simulations that followed.

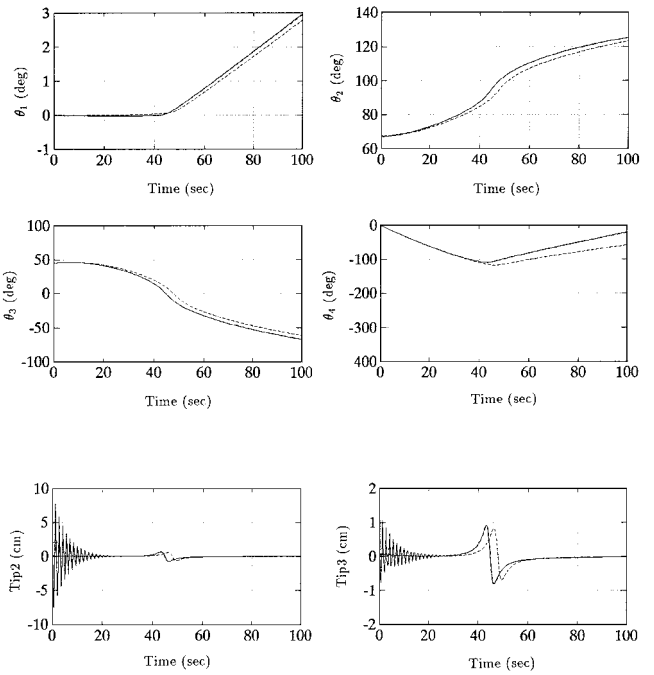

Fig. 3 Uncontrolled postimpact dynamics in the first scenario: joint rotations and tip deflections; ——, hard impact, and – – –, soft impact.

The accuracy of the simulations was ascertained by examining the total energy vs time plot after capture. In the absence of structural damping, the total energy should remain constant. In the presence of structural damping, the total energy reduced, but eventually becomes constant after the oscillations have died out.

As can be observed in Fig. 3, the response for the hard- and soft-impact cases is significantly different, especially the tip deflections. When the relative velocity between the end effector and the grapple point is zero (soft impact), elastic oscillations are not excited. But if there is even a small relative velocity between the two, there can be significant link oscillations and slightly greater joint rotations. The maximum bending moment at the rod is 230 Nm for the first link and 32 Nm for the second, which are tolerable. The response suddenly changes course at about 45 s because at that instant θ_3 goes through zero degree, aligning the two arms and thus putting the manipulator in a singular configuration. This singular configuration introduces a jump in the elastic deflections as well as a significant drift in the spacecraft attitude (θ_1).

The second scenario defined in Fig. 2 is exactly the same as the first, except that now we have a 10-m long flexible appendage hinged to the payload. The results obtained here for $\theta_1 - \theta_4$ are quite similar to those in the first case and are not shown here; in addition, the appendage rotation θ_5 has a tendency to grow after the singular configuration at 45 s (Fig. 4).

From Figs. 3 and 4 it is clear that some form of control is necessary to eliminate the attitude drift of the mother spacecraft and damage to overrotated joint actuators. The control scheme given by Eq. (30) was now applied to the second scenario simulation, the results of which are shown in Figs. 5 and 6. The joint angles have been brought back to their initial values within 20 s. The applied control torques (Fig. 6) are quite reasonable, with the highest torque required after the hard impact is about 40 Nm. However, the torques excite elastic oscillations of the links (which are uncontrolled).

The last scenario corresponds to the docking of the shuttle with the space station in its early phase assisted by the Space Station Remote Manipulator Systems (SSRMS). The parameters used in the simulation are given in Table 2. The motion is confined to the orbital plane of the space station. The base of the SSRMS is at a distance of 1 m from the center of mass of the space station, whereas the grapple point of the shuttle is 5 m away from its center of mass. Figure 7 shows the results for the case when the shuttle has a rotational rate of 0.5 rpm and the grapple point has a relative velocity of 0.1 m/s with respect to the SSRMS end effector. The assumption is made that the capture is successful, i.e., the impact is

Table 2 Parameters for the space station-shuttle docking simulation

Body	l, m	m, kg	EI, N-m^2	J_{zz}, kg-m^2
Space station	n/a	150,000	n/a	60×10^5
Link 1	7.5	200	38×10^5	n/a
Link 2	7.5	200	38×10^5	n/a
Shuttle	n/a	60,000	n/a	10×10^6

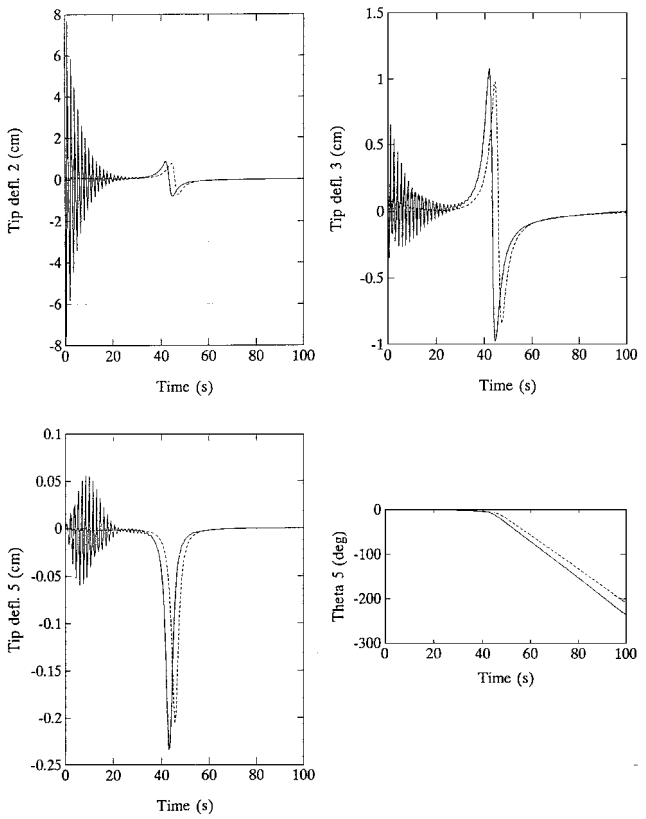

Fig. 4 Uncontrolled postimpact dynamics in the second scenario: θ_5 and tip deflections; ——, hard impact, and – – –, soft impact.

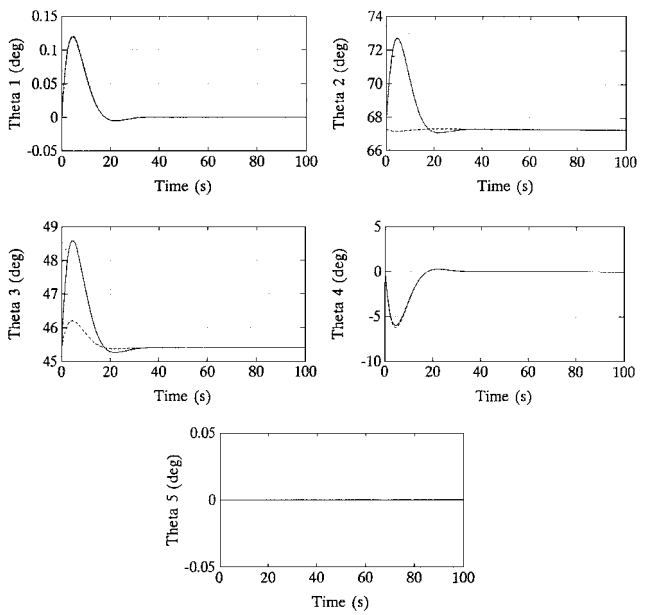

Fig. 5 Controlled postimpact dynamics in the second scenario: joint rotations; ——, hard impact, and – – –, soft impact.

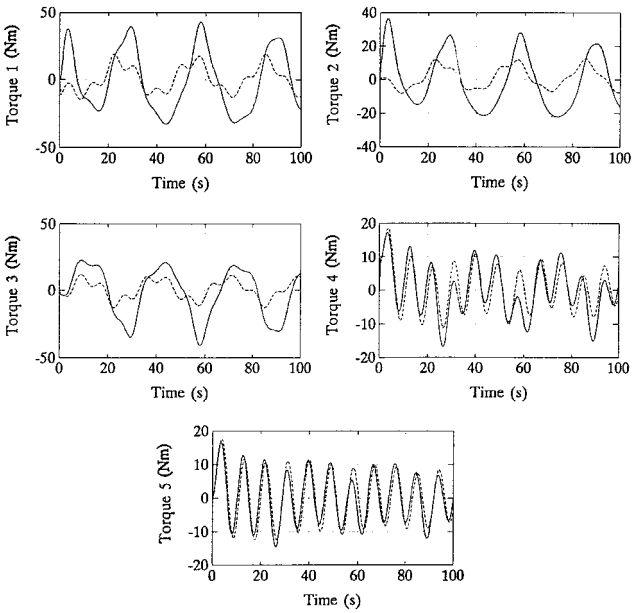

Fig. 6 Control toruqes in the second scenario: ——, hard impact, and – – –, soft impact.

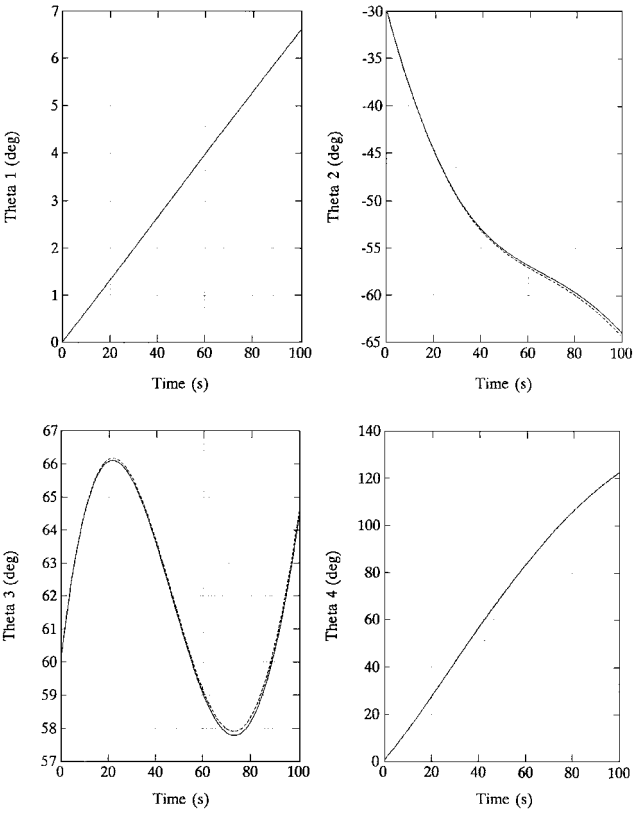

Fig. 7 Uncontrolled space station—shuttle docking simulation: ——, hard impact, and – – –, soft impact.

a plastic one. After the impact the space station's attitude drifts, the pitch angle reaching approximately 6.6 deg after 100 s. This large drift can be explained by the fact that the moment of inertia of the shuttle is quite significant compared to that of the space station in its early phase of construction. The SSRMS link-tip deflections are very small and are not shown. The maximum bending moment is about 15 Nm because of the relatively high flexural rigidity of the links. The rotations of the links, on the other hand, are quite large and may be unacceptable. Figure 8 presents the dynamic behavior for the controlled case. Although the control is successful, the torques required are of the order 10^5 Nm and are larger for the hard-impact case.

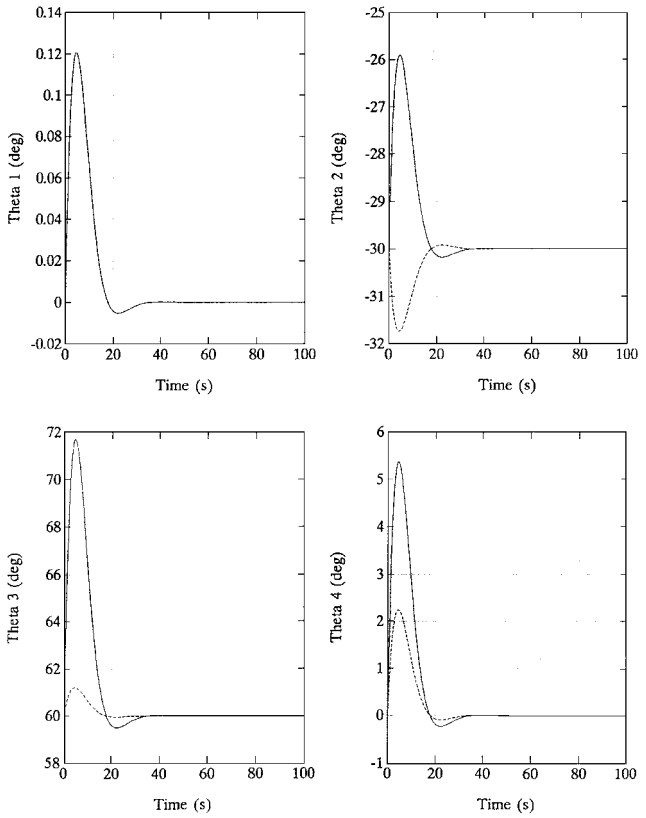

Fig. 8 Controlled space station—shuttle docking simulation: ——, hard impact, and – – –, soft impact.

Conclusion

In this paper the postimpact dynamics of a space manipulator capturing a satellite payload with a flexible appendage is modeled and simulated. Both cases of a flexible and rigid manipulator impacting the payload have been considered. A method was presented to determine the initial conditions for postimpact simulation. The simulation results show that consideration of impact loading in the dynamics and control study of payload capture is important and must be taken into consideration. The models developed here can be easily adapted to two colliding multibody systems in orbit.

Acknowledgments

The authors wish to express their gratitude to the Institute of Robotic and Intelligent Systems Network and the Natural Sciences and Engineering Research Council of Canada for providing the funding for this research.

References

[1]Umetani, Y., and Yoshida, K., "Resolved Motion Rate Control of Space Manipulators with Generalized Jacobian Matrix," *IEEE Transactions on Robotics and Automation*, Vol. 5, No. 3, 1989, pp. 303–314.

[2]Umetani, Y., and Yoshida, K., "Experimental Study on Two Dimensional Free-Flying Robot Satellite Model," *Proceedings of the NASA Conference on Space Telerobotics*, Jet Propulsion Lab., Pasadena, CA, 1989.

[3]Longman, R. W., "Attitude Tumbling Due to the Flexibility in Satellite-Mounted Robots," *The Journal of Astronautical Sciences*, Vol. 38, No. 4, 1990, pp. 487–509.

[4]Baruh, H., and Tadikunda, S. S. K., "Issues in the Dynamics and Control of Flexible Robot Manipulators," *AIAA Symposium on Dynamics and Control of Large Space Structures*, edited by L. Meirovitch, AIAA, New York, 1987, pp. 659–671.

[5]Papadopoulos, E., and Dubowsky, S., "On the Nature of Control Algorithms for Free-Floating Space Manipulators," *IEEE Transactions on Robotic and Automation*, Vol. 7, No. 6, 1991, pp. 750–758.

[6]Dubowsky, S., Vance, E., and Torres, M., "The Control of Space Manipulators Subject to Spacecraft Attitude Control Saturation Limits," *Proceedings of the NASA Conference on Space Telerobotics*, Jet Propulsion Lab., Pasadena, CA, 1989.

[7]Torres, M., and Dubowsky, S., "Path Planning for Space Manipulators to Minimize Spacecraft Attitude Disturbance," *Proceedings 1991 IEEE International Conference on Robotics and Automation*, Vol. 3, IEEE Publications, Piscataway, NJ, 1991, pp. 2522–2528.

[8]Longman, R., Lindberg, R., and Zeed, M., "Satellite-Mounted Robot Manipulators—New Kinematics and Reaction Moment Compensation," *International Journal of Robotics Research*, Vol. 6, No. 3, 1987, pp. 87–103.

[9]Vafa, Z., and Dubowsky, S., "On the Dynamics of Space Manipulators Using the Virtual Manipulator, with Application to Path Planning," *The Journal of Astronautical Sciences*, Vol. 38, No. 4, 1990, pp. 441–472.

[10]Wang, Y., and Mason, M., "Modeling Impact Dynamics for Robotic Operations," *Proceedings 1987 IEEE International Conference on Robotics and Automation*, Vol. 2, IEEE Publications, Piscataway, NJ, 1987, pp. 678–685.

[11]Yoshida, K., Kurazume, R., Sashida, N., and Umetani, Y., "Modelling of Collision Dynamics for Space Free-Floating Links Extended Generalized Inertia Tensor," *Proceedings 1992 IEEE International Conference on Robotics and Automation*, IEEE, Piscataway, NJ, 1992, pp. 899–904.

[12]Yoshida, K., "Impact Dynamics Representation and Control with Extended-Inversed Inertia Tensor for Space Manipulators," *Robotics Research*, Vol. 6, 1994, pp. 453–463.

[13]Carton, D., Chretien, J. P., and Maurette, M., "Dynamics Modelling and Control of a Flexible Arm Holding a Non-Rigid Payload," *Proceedings of the 2nd European In-Orbit Operations Technology Symposium*, Toulouse, France, 1989.

[14]Cyril, X., Jaar, G. J., and Misra, A. K., "Dynamical Modelling and Control of a Spacecraft-Mounted Manipulator Capturing a Spinning Satellite," *Acta Astronautica*, Vol. 35, No. 2/3, 1995, pp. 167–174.

[15]Cyril, X., Angeles, J., and Misra, A. K., "Dynamics of Flexible Multi-Body Mechanical Systems," *Transactions of the CSME*, Vol. 15, No. 3, 1991, pp. 235–256.